

Anomalous Power Flow and “Ghost” Sources

Cesar Monzon

Enig Associates, Inc., Silver Spring, Maryland 20904, USA

(Received 8 March 2006; revised manuscript received 21 July 2008; published 20 August 2008)

It is demonstrated that EM radiation from complex sources can result in real power in restricted regions of space flowing back towards the sources, thereby mimicking “ghost” sources. This counterintuitive mechanism of radiation does not rely on backward waves, as ordinary waves carry the power. Ways to harness the effect by making it directional are presented, together with selected applications, of which deception is a prime example due to the nature of the phenomenon. The concept can be applied to other areas, such as mechanics, acoustics, etc., and can be realized with available technology.

DOI: 10.1103/PhysRevLett.101.083901

PACS numbers: 41.20.Jb, 42.25.Fx, 42.25.Hz

It is typically assumed that given a distribution of electromagnetic (EM) radiators, power always travels away from the radiators [1–6]. Particularly, average power measurements in the surrounding area of radiators are universally interpreted as a measure of the strength of the sources [7,8]. This is an intuitive picture, reinforced by the common notion of a uniformly illuminated aperture, or an antenna phase array, where power always flows away from the structure [9,10]. We have found that, counterintuitively, this is not always the case, and that under some special conditions of geometry, location, and frequency, power may flow back in the direction of the sources. Here, we demonstrate theoretically and through simulations that reverse power flow does not violate the field equations. It should be clarified that we are talking about real power flow, and not reactive power flow, as the latter is of no significance to us here.

The principle will be presented via a simplified representation of the radiated field from a collection of sources. The time convention $\exp(-i\omega t)$ is assumed. For the case of cylindrical waves (i.e., two dimensional), a distribution of filamentary currents $I\hat{z}$, located on the $x = 0$ plane, and separated by a distance d in the y direction, produces a z -directed E field [1]

$$E(\bar{x}) = -\frac{\omega\mu_0 I}{4} \sum_{-\infty}^{\infty} H_0^{(1)}(k_0|\bar{x} - nd\hat{y}|). \quad (1)$$

This expression possesses an alternative spectral representation, which can also be used to obtain the real radiated power everywhere via the standard form [1] $\bar{P} = \text{Re}\{\bar{E} \times \bar{H}^*\}$. Alternatively, we can use a variety of commercial software to accomplish this. For compatibility with more complicated geometries that follows, we decided to use HFSS (Ansoft). The power \bar{P} flow pattern is presented in Fig. 1, which corresponds to $d = 2.8$ cm, and a range of frequencies. Consideration of the vector flow indicates that there is a frequency band where the radiated power right in front of the sources flows back towards the array. And this happens when the source separation is about a wavelength, and the anomalous region where power reverses is roughly half a wavelength away from the array. It should be noted

from Fig. 1(b) that vortex formation accompanies the power reversal.

This remarkable observation is counterintuitive and does not correspond to a fluid dynamic analog, where a nozzle will create eddies that flow along the main direction of power flow, and not against it. And an infinite number of sources is not a requirement. Consider, for example, the case of three identical dipole sources, with currents $I\hat{z}$, and located on the y -axis with a separation d . For (r, θ, ϕ) spherical coordinates centered on a given dipole, the θ -directed single dipole E field, and ϕ directed H field on the $z = 0$ plane ($\theta = \pi/2$) are given by [1]

$$\begin{aligned} E_\theta &= A\eta_0 \left(-\frac{i}{s} + \frac{1}{s^2} + \frac{i}{s^3} \right) \exp(is) \\ H_\phi &= A \left(-\frac{i}{s} + \frac{1}{s^2} \right) \exp(is) \end{aligned} \quad (2)$$

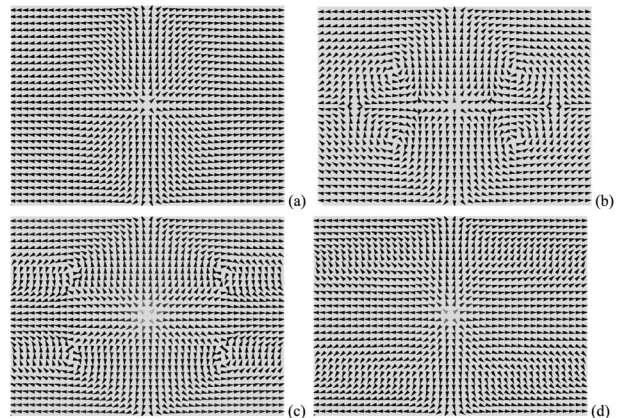


FIG. 1. Radiated power P flow lines for an infinite array of sources aligned along y (vertical). Only one cell is presented, and the filamentary source is located at the center of the area shown, which corresponds to a vertical extent $d = 2.8$ cm, and horizontal (x -directed) coverage 3.8 cm. (a) 8 GHz, (b) 10 GHz, (c) 11 GHz, and (d) 15 GHz. At around 10 GHz, an anomalous power flow pattern develops, where power half a wavelength away from the array flows towards each source, and is accompanied by vortex formation. Away from 10 GHz, a “normal” power flow pattern exists.

where $s = k_0 r$, A the dipole strength, and η_0 the wave impedance. Noted that on the $z = 0$ plane, $E_\theta = E_z$. Superposition gives the field due to the three dipoles, and since the phase terms $\exp(is)$ will have a different effect on E as they do have on H , the phase difference between E and H will be variable depending on location, dipole separation, and frequency. Nothing bounds the phase difference, which results in backward power if it exceeds $\pi/2$. The algebra is tedious, however, after conversion of H_ϕ into H_y , and upon retaining only up to inverse quadratic terms in s (not too close to the array), we obtain the approximate power flow on the x axis,

$$P_x \propto \left\{ \frac{1 + 4(x/q)^3}{2(x/q)(1 + x/q)} + \cos[k_0(q - x)] \right. \\ \left. - \left(\frac{1}{k_0 q} - \frac{1}{k_0 x} \right) \sin[k_0(q - x)] \right\}, \quad (3)$$

where $q = \sqrt{d^2 + x^2}$. If we set $k_0(q - x) = \pi$ in Eq. (3), we have that P_x crosses zero when $q \approx 2x$, and turns negative for x slightly larger than $x \approx \lambda/2$, with corresponding $d \approx 0.9\lambda$. An exact numerical evaluation of P_x reveals that it is negative in the range $0.62\lambda < x < 0.82\lambda$. This is along the lines of what we have seen with the infinite array.

The first term of Eq. (3) is a purely geometric term, which must be overcome by the remaining terms which have a purely electrical character and must be negative for backward power flow to occur. The geometric term is a convex function in x/q , resembling a potential in celestial mechanics, and exhibiting a narrow minimum of 0.97 at $x/q \approx 0.6$, which barely allows for the electrical terms (of order 1) to overcome it. This explains why the effect is narrowband and position dependent. The equation is reminiscent of a mechanical object with kinetic energy (electrical terms) that must be larger than the potential energy (geometrical term) of a barrier in order to overcome it. The situation is illustrated by means of Fig. 2(a) which displays the exact P_x for $d = \lambda = 1$ cm, and dipole sources located at $(2,1,0)$, $(2,2,0)$, and $(2,3,0)$. Under ordinary conditions, $P_x > 0$ for $x > 2$, and $P_x < 0$ for $x < 2$. Since it is difficult

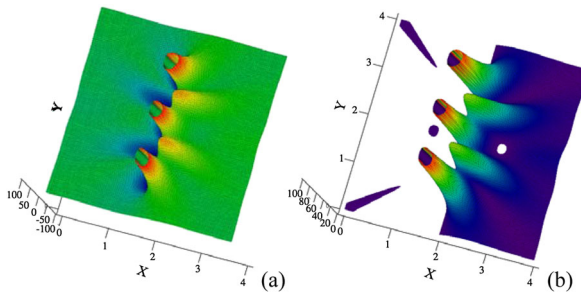


FIG. 2 (color online). Exact power flow P_x for three dipole sources with $d = \lambda = 1$ cm. (a) Unconstrained surface of P_x on both sides of the array, (b) surface of $P_x \geq 0$. The hole and complementary dot locations are the places where backward power flow takes place.

to visualize the values of P_x we are interested in, Fig. 2(b) shows only the positive values of P_x . A hole around $(2.7,2,0)$ and a solid circle on the opposite side $(1.3,2,0)$ reveal backward power flow at those locations, and with just three sources. Negative P_x also shows up in two strips farther away from the sources, but we find that its value is insignificant and that the net \bar{P} are not directed towards the source; hence, they must be dismissed.

It would be more interesting if the effect was unidirectional. According to Eq. (3), the electrical term must overcome the geometrical term; hence, if we make sure the electrical term overcomes the geometrical term on one side of the array, but not on the other, we would have backward power flow on only one side. This can be done by inserting a low reflection material layer on one side of the array so that the electrical length on that side incorporates the phase delay due to the material, and reverses P_x . We have verified this by modifying the original geometry that led to Fig. 1, by inclusion of a 1 mm thick quartz slab of $\epsilon = 4.0$. The HFSS simulation results for $d = 2.8$ cm are presented in Fig. 3, where it can be observed that at 9 GHz, power reversal takes place only on the side opposite to that of the sources.

As expected, away from the critical 9 GHz, the effect is significantly reduced (at 8 GHz there is no trace of this); however, the figure reveals that, at 11 GHz, something noteworthy takes place, power reversal, but in the vicinity

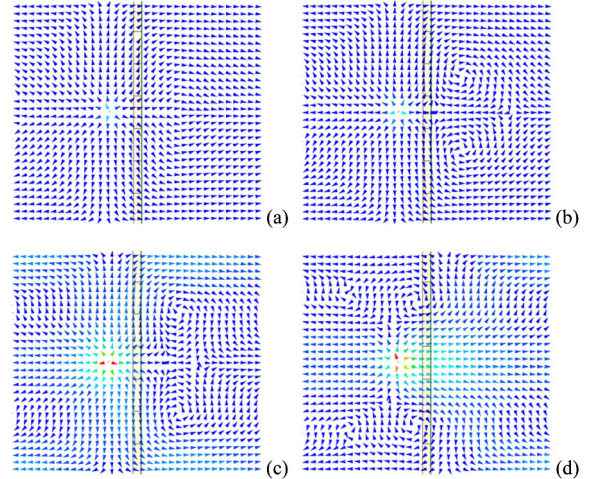


FIG. 3 (color online). Radiated power P flow lines for an infinite array of filamentary sources in the presence of a 1 mm thick quartz slab of $\epsilon = 4.0$. The sources are located on the left of the slab, 3 mm away from the face. Only one cell is shown, and the area corresponds to a vertical extent $d = 2.8$ cm and horizontal (x -directed) coverage 3.1 cm. (a) 8 GHz, (b) 9 GHz, (c) 10 GHz, and (c) 11 GHz. At around 9 GHz, an anomalous power flow pattern develops on the right-hand side, where power flows towards each source, and is accompanied by vortex formation. Away from 10 GHz, a “normal” power flow pattern exists. At 11 GHz, power reversal occurs on the side of the array, but in a less dramatic fashion, in the surroundings of the plane of the sources.

of the plane of the array, which is significantly less dramatic than the effect presented above and possibly not surprising in view of the fact that in an endfire array, power flows against the individual radiators.

It is important to mention that the backward power towards the source is not being carried via a backward wave mechanism, but by an ordinary wave as power and phase flow in the same direction. This is clearly displayed in a plot of the phase of the electric field in the above geometry which includes the 1 mm thick quartz slab. This is presented in Fig. 4 and has been calculated via HFSS [a minus sign was used in the phase, as HFSS uses the $\exp(j\omega t)$ time convention]. The end result at 9 GHz indicates that with origin at the source, and with the exception of the anomalous power flow direction, the phase corresponds to that of an ordinary source (i.e., the phase increases with distance from the source like $\sim ik\rho$). In the anomalous direction, the phase is also anomalous, as the phase progression reverses, but since power flow also reverses, the end result is an ordinary wave.

It is clear that back power flow is the result of collective interference, wherein the effect of the sources superposes in a way that the gradient of phase (collinear with the phase velocity) in the region in question points backwards towards the source. Since we are not dealing with backward waves, phase velocity, group velocity, and power point in the same direction. It follows that if conditions are favorable, power will locally flow back towards the sources. It should be mentioned that in the literature, power flow towards a source has only been encountered in the context of backward waves, such as in the neighborhood of a log-

periodic antenna [10], or in conjunction with a grounded left handed media (LHM) slab [11].

Above, we have considered independent sources. Sometimes this is not the case, as it occurs with a corporate feed, where power from a main source is divided in balanced arms as the wave progresses, resulting in a series of apertures with (ideally) identical fields. From what has

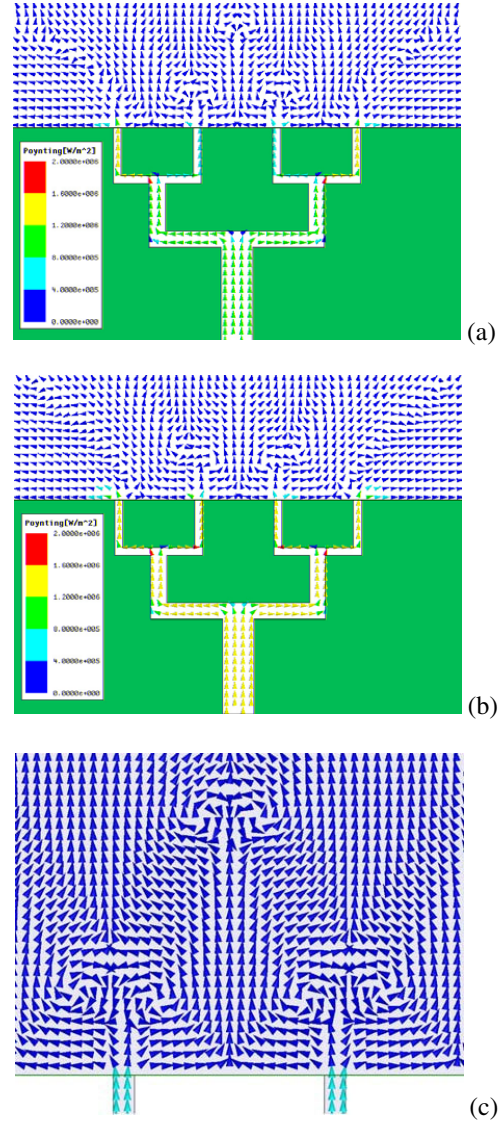


FIG. 5 (color online). Radiated power P flow lines for a four element corporate feed with 0.5" separation between apertures. Operation is at (a) 21 GHz and (b) 22 GHz. The back power flow effect is apparent at 21 GHz, both from the external vector direction, and from the power unbalance on the different arms. At 20 GHz (not shown) and 22 GHz, the power distribution in the different arms is pretty much uniform. (c) Detail of the 21 GHz P flow lines in the neighborhood of the central elements showing expected backward power regions plus an additional backward power region in the central plane, roughly a wavelength away from the aperture plane (note that the power in this region is pointing towards the aperture plane not towards the sources).

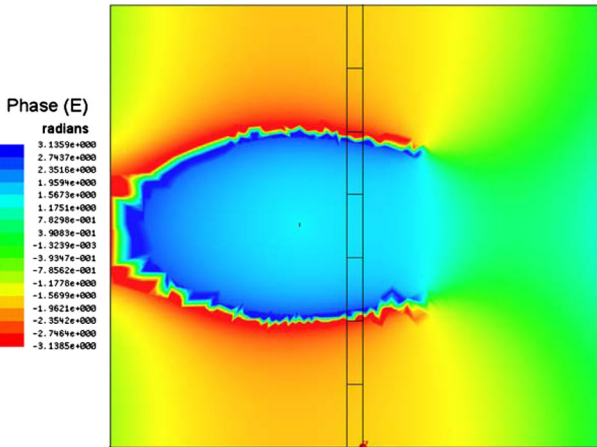


FIG. 4 (color online). Phase of electric field radiated by a 9 GHz infinite array of filamentary sources in the presence of a 1 mm thick quartz slab of $\epsilon = 4.0$. The sources are located on the left of the slab, 3 mm away from the face. Only one cell is shown, of area 2.8 cm (vertical) by 3.1 cm (horizontal). HFSS generated phase distribution indicates that backward power is not carried by backward wave means. The anomalous phase shown in the direction of anomalous power flow [see Fig. 3(b)] result in ordinary wave propagation everywhere.

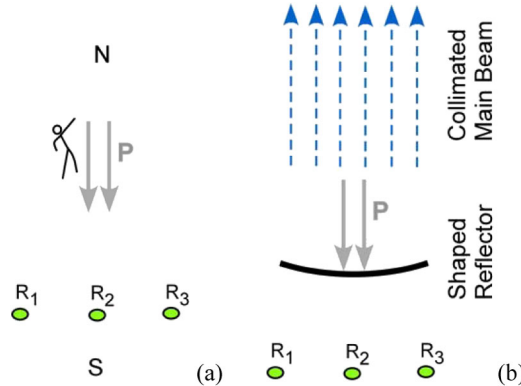


FIG. 6 (color online). Potential applications of “ghost” sources. (a) Deception, making believe an observer that we are in the North when in reality we are in the South; (b) creating a “ghost” feed for a shaped reflector in order to create a high gain antenna. The R’s denote a number of properly designed radiating sources.

been said above, when the frequency is such that the separation between apertures is of the order of a wavelength, we expect that at roughly half a wavelength away from the central aperture(s), power will exhibit a tendency towards backward flow, opposing the power coming out of the aperture. For a corporate feed, however, the effect will result in a significant reduction in the amount of power coming out of the affected aperture(s), with consequent redirection of power towards the other apertures (note that this is not the typical scenario, as radiators are usually spaced less than half a wavelength apart in order to avoid grating lobes). Figure 5 illustrates a basic corporate feed with four arms, where a 0.5” aperture separation led to backward power flow at 21 GHz. No significant effect was observed at 20 and 22 GHz (shown in the Figure). The effect is not as evident in the exterior of the array, as with the case of independent sources, because now the backward power does affect the source itself. The effect is however clear from consideration of the power levels at the different arms, which exhibit marked contrast, a significant reduction in the central arms (about half the power of the outer arms).

An important thing to be noticed in Fig. 5(c) is the appearance of an extra backward power region in the central plane, located roughly a wavelength away from the aperture plane. A unique tree formation results due to suitable fields at the aperture plane of the corporate feed. This does not happen for a very large number of apertures (the infinite array of sources was rerun to check this, unsuccessfully). This means that proper design can lead to at-will placement.

Although explainable through classical means, this is an unexpected physical phenomenon which opens up the possibility of a plethora of applications, deception being one of them; we can design an array of sources in a way that we make an observer believe (through measurements) that we are in the North, when in reality we are in the South. Or we can create “ghost” feeds that will feed for instance a dish antenna, resulting in a collimated far field without the need for a real physical feed. Figure 6 illustrates these two applications. The reader should be cautioned that although feasible with current technology, turning these and other new concepts into reality may require significant developments, just like any major departure from the technological status quo, as exemplified by the case of LHM.

To summarize, we have demonstrated analytically and numerically that EM radiation from complex sources can result in real power in restricted frequency bands and regions of space, flowing back in the direction of the sources. Locally the effect is that of ghost sources. The novel mechanism of radiation does not rely on backward waves, as it is built on interference, and can be made directional in combination with ordinary dielectric structures. This opens up a wealth of applications, of which deception and antenna feeds are prime examples. The concept can be applied to other areas, such as Optics, Acoustics, water wave problems, etc., where it can be realized with available technology.

- [1] R. F. Harrington, *Time Harmonic Electromagnetic Fields* (McGraw-Hill, New York, 1961).
- [2] D. S. Jones, *The Theory of Electromagnetism* (MacMillan, New York, 1964).
- [3] J. D. Jackson, *Classical Electrodynamics* (Wiley, New York, 1999), 3rd ed..
- [4] L. B. Felsen and N. Marcuvitz, *Radiation and Scattering of Waves* (Prentice-Hall, New York, 1978).
- [5] A. Sommerfeld, *Lectures on Theoretical Physics Optics* Vol. 4 (Academic Press, New York, 1954).
- [6] P. M. Morse and H. Feshbach, *Methods of Theoretical Physics* (McGraw-Hill, New York, 1953).
- [7] *Radar Cross Section Handbook* G. T. Ruck (Plenum Press, New York, 1970).
- [8] E. F. Knott, J. F. Shaeffer, and M. T. Tuley, *Radar Cross Section* (SciTech Publishing, New York, 2004), 2nd ed..
- [9] B. Munk, *Finite Antenna Arrays and FSS* (Wiley-IEEE Press, New York, 2003).
- [10] T. A. Milligan, *Modern Antenna Design* (Wiley-IEEE Press, New York, 2004), 2nd ed..
- [11] J. Schelleng, C. Monzon, P. F. Loschialpo, D. W. Forester, and L. N. Medgyesi-Mitschang, Phys. Rev. E **70**, 066606 (2004).